

1 **The NASA Airborne Tropical Tropopause Experiment (ATTREX):**

2 **High-Altitude Aircraft Measurements in the Tropical Western Pacific**

3 Eric J. Jensen\*, Leonhard Pfister, David E. Jordan, and Thaopaul V. Bui, Rei Ueyama, Hanwant

4 B. Singh

5 *NASA Ames Research Center, Moffett Field, California*

6 Troy Thornberry and Andrew W. Rollins

7 *NOAA Earth Science Research Laboratory and Cooperative Institute for Research in*

8 *Environmental Science, Boulder, CO, USA*

9 Ru-Shan Gao, David W. Fahey, Karen H. Rosenlof, and James W. Elkins

10 *NOAA Earth Science Research Laboratory, Boulder, CO, USA*

11 Glenn S. Diskin and Joshua P. DiGangi

12 *NASA Langley Research Center, Hampton, VA, USA*

13 R. Paul Lawson and Sarah Woods

14 *Spec Inc., Boulder, CO, USA*

15 Elliot L. Atlas and Maria A. Navarro Rodriguez

16 *University of Miami, Miami, FL, USA*

17 Steven C. Wofsy and Jasna Pittman

18 *Harvard University, Cambridge, MA, USA*

19 Charles G. Bardeen

20 *National Center for Atmospheric Research, Boulder, CO, USA*

21 Owen B. Toon and Bruce C. Kindel

22 *University of Colorado, Boulder, CO, USA*

23 Paul A. Newman and Matthew J. McGill

24 *NASA Goddard Space Flight Center, Greenbelt, MD, USA*

25 Dennis L. Hlavka

26 *Science Systems and Applications, Inc., Greenbelt, MD, USA*

27 Leslie R. Lait

28 *Morgan State University, Baltimore, MD, USA*

29 Mark R. Schoeberl

30 *Science and Technology Corporation, Columbia, MD, USA*

31 John W. Bergman

32 *Bay Area Environmental Research Institute, Sonoma, CA, USA*

33 Henry B. Selkirk

34 *University Space Research Association, Greenbelt, MD, USA*

35 M. Joan Alexander and Ji-Eun Kim

36 *NorthWest Research Associates, CoRA Office, Boulder, CO, USA*

37

Boon H. Lim

38

*Jet Propulsion Laboratory, Pasadena, CA, USA*

39

Jochen Stutz

40

*University of California, Los Angeles, CA, USA*

41

Klaus Pfeilsticker

42

*University of Heidelberg, Heidelberg, Germany*

43 *\*Corresponding author address: NASA Ames Research Center, MS 245-5, Moffett Field, CA*

44 *94035.*

45 *E-mail: [eric.j.jensen@nasa.gov](mailto:eric.j.jensen@nasa.gov)*

## ABSTRACT

46 The February through March 2014 deployment of the NASA Airborne Tropo-  
47 ical TRopopause EXperiment (ATTREX) provided unique in situ measure-  
48 ments in the western Pacific Tropical Tropopause Layer (TTL). Six flights  
49 were conducted from Guam with the long-range, high-altitude, unmanned  
50 Global Hawk aircraft. The ATTREX Global Hawk payload provided mea-  
51 surements of water vapor, meteorological conditions, cloud properties, tracer  
52 and chemical radical concentrations, and radiative fluxes. The campaign was  
53 partially coincident with the CONTRAST and CAST airborne campaigns  
54 based in Guam using lower-altitude aircraft (see companion articles in this  
55 issue). The ATTREX dataset is being used for investigations of TTL cloud,  
56 transport, dynamical, and chemical processes as well as for evaluation and im-  
57 provement of global-model representations of TTL processes. The ATTREX  
58 data is openly available at <https://espoarchive.nasa.gov/>.

## 59 1. Introduction

60 The NASA Airborne Tropical Tropopause EXperiment (ATTREX) was a five-year airborne  
61 science program focused on the physical processes occurring in the Tropical Tropopause Layer  
62 (TTL,  $\approx 13\text{--}19$  km). Inasmuch as the Brewer-Dobson circulation transports air upward through the  
63 TTL and then throughout the entire stratosphere, processes controlling TTL composition provide a  
64 boundary condition for stratospheric composition. A particular focus of ATTREX is the dehydra-  
65 tion of air entering the stratosphere by ice crystal growth and sedimentation near the cold tropical  
66 tropopause. Radiative transfer calculations show that even small changes in stratospheric humid-  
67 ity have climate impacts that are significant compared to those of decadal increases in greenhouse  
68 gases (??). While the tropospheric water vapor-climate feedback is well represented in global  
69 models, predictions of future changes in stratospheric humidity are highly uncertain because of  
70 gaps in our understanding of physical processes occurring in the TTL. Uncertainties in the TTL  
71 transport processes and chemical composition also limit our ability to predict future changes in  
72 stratospheric ozone. The 2014 ATTREX deployment to Guam was particularly valuable for ad-  
73 dressing these science issues given that the lowest tropopause temperatures, driest TTL air, and  
74 strongest upward transport occur in the western Pacific during Boreal wintertime.

75 Stratospheric humidity and chemical composition are controlled by a complex interplay of pro-  
76 cesses occurring in the TTL (Figure 1). Deep convection links surface conditions to the upper  
77 troposphere. The strength and depth of convection impacts transport of water vapor and chemical  
78 constituents to the TTL and deep convection is the predominant source of tropical waves. Trop-  
79 ical waves affect TTL thermal structure cirrus formation and wave breaking and dissipation in  
80 the stratosphere drive large scale ascent in the tropics. Ubiquitous TTL cirrus have a direct effect  
81 on the Earth's radiation budget, and their regulation of stratospheric humidity results in an indi-

82 rect radiative effect. TTL processes also influence the stratospheric ozone layer. Since precursors  
83 of ozone-depleting substances pass through the TTL before reaching the stratosphere, the TTL  
84 composition has a controlling influence on rates of stratospheric ozone destruction (?).

85 The ATTREX campaigns used the long-range (16,000 km), high-altitude (20 km) NASA Global  
86 Hawk unmanned aircraft system for TTL measurements (Figure 2). The ATTREX Global Hawk  
87 payload consisted of twelve instruments measuring cloud properties, water vapor, meteorological  
88 conditions, chemical tracers, chemical radicals, and radiation (see Table 1). The overall ATTREX  
89 project was managed by the NASA Ames Research Center, and the Global Hawk program is  
90 managed by Armstrong Flight Research Center (AFRC, formerly Dryden Flight Research Cen-  
91 ter). Prior to the Guam deployment, two ATTREX flight series were conducted out of AFRC,  
92 providing measurements in the central and eastern Pacific TTL (see ? for details). We report here  
93 on the January–March, 2014 ATTREX deployment to Guam (13°28'0" N, 144°46'59" E), which  
94 provided measurements in the western Pacific.

## 95 **2. ATTREX Global Hawk Payload**

96 The ATTREX payload was designed to address key uncertainties in our understanding of TTL  
97 composition, transport, and cloud processes affecting water vapor and short-lived trace gases.  
98 Measurements of water vapor, cloud properties, numerous chemical tracers, key radical species,  
99 meteorological conditions, and radiative fluxes were included (Table 1). Instruments were chosen  
100 based on proven techniques and size/weight accommodation on the Global Hawk.

101 The very dry conditions present in the tropical tropopause region ( $\text{H}_2\text{O}$  mixing ratios as low  
102 as  $\simeq 1$  ppmv) represent a significant challenge for accurately measuring water vapor. Large, unre-  
103 solved discrepancies between past water vapor concentrations measured with different instruments

104 (??) have generally precluded use of the measurements for detailed studies of cloud microphysical  
105 processes.

106 The water vapor measurement challenges were addressed in ATTREX by including two com-  
107plementary instruments, namely Diode Laser Hygrometer (DLH) and NOAA Water (NW), both  
108of which have suitable sensitivity for measuring water vapor values as low as 1 ppmv. The NW  
109instrument (added to the payload in 2013) provides a closed-cell tunable-diode laser (TDL) mea-  
110surement that includes the in-flight calibration system used on the NOAA chemical ionization  
111mass spectrometer (CIMS) instrument during MACPEX (?). Calibration during the flights avoids  
112the uncertainty associated with assuming that ground-based calibrations apply to in-flight condi-  
113tions. The NW instrument also measures total water concentration using a forward-facing inlet  
114that enhances ice concentration. The DLH instrument provides an open-path TDL measurement  
115by firing the laser from the fuselage to a reflector on the wing and measuring the return signal. The  
116path length (12.2 m) is long enough to provide a precise, fast measurement of water vapor. The  
117precision is sufficient to permit detection of fine structure in the TTL water vapor field even at a  
118data rate approaching 100 Hz. With typical flights speeds of  $170 \text{ m s}^{-1}$  and ascent/descent rates  
119of  $10 \text{ m s}^{-1}$ , DLH provides measurements with spatial resolution determined by the geometry  
120of its optical path: about 6 m horizontally and less than 0.5 m vertically. Temperature, pressure,  
121and wind measurements were made with the Meteorological Measurement System (MMS) that  
122also provided high-frequency data (up to 20 Hz) and permits examinations of fine structures in the  
123relative humidity field and their correlation with cloud variations (?).

124 We have a high level of confidence in the estimated accuracy of the DLH and NW measurements  
125( $\simeq 5\text{--}10\%$ ) for two reasons: (1) The NW and DLH data obtained in the 2013 and 2014 flights show  
126a high degree of consistency and agreement for TTL  $\text{H}_2\text{O}$  values less than 10 ppmv (see Figure 7).  
127(2) In TTL cirrus with very high ice concentrations (in excess of  $1 \text{ cm}^{-3}$ ) the relative humidity

128 with respect to ice ( $RH_{ice}$ ) is consistently near 100% (?). The time scale for quenching of super-  
129 /sub-saturation by ice crystal growth/sublimation in such clouds is a few minutes or less such that  
130 the  $RH_{ice}$  is expected to remain near 100%.

131 For the Guam ATTREX flights, TTL cirrus microphysical properties were measured with the  
132 Spec Inc. Hawkeye instrument. Hawkeye is a combination of two imaging instruments (equiv-  
133 alent to the two-dimensional Stereo probe (2D-S) (?) and Cloud Particle Imager (CPI) (?)), and  
134 a spectrometer (equivalent to the Fast Cloud Droplet Probe (FCDP) (?)), all of which have been  
135 used in the past for airborne cloud measurements. For consistency and comparison with the 2011  
136 and 2013 ATTREX flight series, a stand-alone FCDP was also included in the Guam payload. The  
137 combination of FCDP and 2D-S probes provides ice crystal size distributions spanning crystal  
138 maximum dimensions from about 1  $\mu\text{m}$  to about 4 mm. The CPI provides detailed ice crystal im-  
139 ages that can be used to determine habit information for crystals with maximum dimensions larger  
140 than about 40  $\mu\text{m}$ . The cloud measurements, along with the water vapor and temperature measure-  
141 ments, are being used to test our theoretical understanding of ice crystal nucleation, depositional  
142 growth, and sedimentation (e.g. ???).

143 The ATTREX payload included a number of tracer measurements that can be used to quan-  
144 tify TTL transport pathways and time scales. The Harvard University Picarro Cavity Ringdown  
145 System (HUPCRS) provides precise, stable measurements of  $\text{CO}_2$  and  $\text{CH}_4$ . The HUPCRS also  
146 includes a CO channel that provides useful data with some averaging. The UAS Chromatograph  
147 for Atmospheric Trace Species (UCATS) provides measurements of  $\text{O}_3$ ,  $\text{N}_2\text{O}$ ,  $\text{SF}_6$ ,  $\text{H}_2$ , CO (tro-  
148 pospheric), and  $\text{CH}_4$ , as well as an additional measurement of water vapor.

149 The Global Hawk Whole Air Sampler (GWAS) provides 90 gas canister samples per flight. The  
150 times for the GWAS samples were determined on a real-time basis depending on the flight plan.  
151 Post-flight, gas chromatographic analysis provides concentrations of a plethora of trace gases with

152 sources from industrial mid-latitude emissions, biomass burning, and the marine boundary layer,  
153 with certain compounds (e.g. organic nitrates) that have a unique source in the equatorial surface  
154 ocean. GWAS also measures a full suite of halocarbons that provide information on the role of  
155 short-lived halocarbons on chemistry in the tropical UTLS region, on halogen budgets in the UTLS  
156 region, and on trends of HCFCs, CFCs, and halogenated solvents.

157 The ATTREX payload also included radiation measurements, which will be used to quantify  
158 the impacts of clouds and water vapor variability on TTL radiative fluxes and heating rates. The  
159 spectral solar flux radiometer (SSFR) measurements additionally provide information about cir-  
160 rus microphysical properties, and retrieval of TTL water vapor amounts with SSFR spectra has  
161 been demonstrated (?). Lastly, the Differential Optical Absorption Spectrometer (mini-DOAS)  
162 instrument provides measurements of BrO, NO<sub>2</sub>, O<sub>3</sub>, IO, O<sub>4</sub>, H<sub>2</sub>O, and cloud/aerosol extinction  
163 at various elevation angles near the limb. These measurements can be converted to vertical trace  
164 gas concentration profiles from 1 km above to 5 km below flight altitude using radiative transfer  
165 calculations and either optimal estimation or O<sub>3</sub> absorption techniques. The combination of the  
166 mini-DOAS BrO (and IO) measurements and GWAS measurements of major halogenated hydro-  
167 carbons provides constraints on the TTL and lower stratospheric Br<sub>y</sub> and I<sub>y</sub> budgets.

168 Two additional remote-sensing instruments were included that provide both valuable sci-  
169 ence data and real-time information for flight operations. The Cloud Physics Lidar (CPL) provides  
170 profiles of aerosol/cloud backscatter and depolarization below the aircraft. The high sensitivity of  
171 CPL backscatter measurements have proven useful for detecting tenuous TTL cirrus (?), and the  
172 depolarization measurement provides information about ice crystal habits. The Microwave Tem-  
173 perature Profiler (MTP) provides vertical profiles of temperature above and below the aircraft. The  
174 CPL and MTP data was transmitted to the Global Hawk ground operations center via a high-speed

175 data link, and the information was used to determine when to execute vertical profiles through the  
176 TTL.

### 177 **3. ATTREX 2014 Global Hawk Flights**

178 The overall ATTREX project included multiple campaigns: flights were conducted out of AFRC  
179 in the fall of 2011 and the winter-spring of 2013 (see ? for details). Here, we report on the  
180 2014 deployment to Guam in the western Pacific during February and early March, 2014. The  
181 flight paths for the six Guam Global Hawk flights are shown in Figure 3, along with the earlier  
182 ATTREX flights for context. The Coordinated Airborne Studies in the Tropics (CAST) and the  
183 CONvective TRansport of Active Species in the Tropics (CONTRAST) campaigns were planned  
184 to be concurrent with the ATTREX Guam flights. The CAST and CONTRAST campaigns are  
185 described in separate articles in this issue. A series of aircraft operations problems delayed the  
186 Global Hawk flights until the CAST and CONTRAST operations were essentially completed.  
187 Nevertheless, the combined lower- to middle-troposphere sampling from CAST and CONTRAST  
188 flights and upper troposphere/lower stratosphere ATTREX Global Hawk measurements provide  
189 unique information about the western tropical Pacific atmospheric composition from the surface  
190 to the stratosphere.

191 The Guam flights provided an extensive survey of western Pacific TTL composition. Details of  
192 the individual Global Hawk flights from Guam are provided in Table 2. The general sampling strat-  
193 egy was to execute numerous vertical profiles between 45,000 ft ( $\simeq$ 13.7 km) and cruise altitude  
194 (53,000–60,000 ft ( $\simeq$ 16.2–18.3 km), depending on the fuel load). Figure 4 shows the resulting  
195 coverage in longitude, latitude, and height space. Global Hawk power constraints forced us to turn  
196 off the GWAS pumps on descents; thus, GWAS samples were taken during the ascents only.

197 The transit from AFRC to Guam on 16–17 January, 2014 served primarily to transport the Global  
198 Hawk to the deployment location. Concerns about fuel consumption and limited ability to transmit  
199 commands to the aircraft payload during the flight precluded execution of vertical profiles through  
200 the TTL. The aircraft cruised near the tropical tropopause for most of the flight. As mentioned  
201 above, aircraft operational and mechanical problems (as well as unusually severe local weather  
202 in Guam) prevented Global Hawk flights for the next several weeks after arrival in Guam while  
203 CONTRAST and CAST were underway.

204 The prevailing meteorological pattern in the Boreal winter western Pacific TTL has a pool of  
205 cold temperatures located just east of the most active convection (?) (see Figure 3). These cold  
206 temperatures are essentially a wave response to the convective heating and uplift; as part of this  
207 wave response, there is a Boreal hemisphere anticyclone, usually centered north and slightly east  
208 of the cold temperature pool. There is frequently a corresponding anticyclone in the southern  
209 hemisphere, though this was typically out of range of ATTREX sampling. The convection (which  
210 is strongest in the southern hemisphere during Boreal winter, though there is significant penetration  
211 to northern hemisphere latitudes – Figure 3) is modulated by the Madden-Julian Oscillation (MJO,  
212 (?)). This oscillation produces substantial fluctuations in the position and intensity of the cold  
213 temperature pool and the associated anticyclone. The primary research flights occurred during the  
214 period 12 February through 13 March, during which time the cold pool and anticyclone basically  
215 moved from well west of Guam to the central Pacific, roughly consistent with the propagation  
216 of the MJO. The progression of the center of the anticyclone with the various research flights is  
217 shown by the “X” symbols in Figure 3.

218 The first ATTREX local flight from Guam (RF01) occurred on 12-13 February. The primary  
219 focus of this flight was to survey the composition, humidity, clouds, and thermal structure of the  
220 western Pacific TTL. During this flight, convection was most active well west of Guam and sup-

221 pressed at Guam's longitudes, so the center of monsoon anticyclone (Figure 3) and the coldest  
222 TTL temperatures were also west of Guam. A semi-Lagrangian flight plan, approximately along  
223 the streamlines of the anticyclone was chosen, arcing north and west of Guam, and then reversing  
224 course and heading south of Guam down to near the equator. Limitations on Global Hawk opera-  
225 tions in cold temperatures and aerodynamic drag prevented the aircraft from climbing above about  
226 57,000 ft (17.8 km). Cirrus clouds were observed throughout the TTL, almost certainly formed in  
227 situ because of the absence of nearby convection. Given the westward position of the anticyclone,  
228 the TTL circulation was from the west northwest, and back trajectory analysis showed that a sig-  
229 nificant portion of the air sampled had progressed clockwise around the anticyclone after having  
230 been detrained from convective systems in Africa about a week to 10 days prior to the time of ob-  
231 servation. The CO<sub>2</sub> and methane measurements were consistent with this picture. The trajectory  
232 method used is similar to that described in ? and ?. That is, diabatic back trajectories are calcu-  
233 lated from clusters of points surrounding the aircraft measurements using ERA-Interim analyses  
234 and observed diabatic heating rates typical for the Boreal winter season (?). These back trajectories  
235 are routed through 3-hourly fields of cloud top potential temperature derived from global infrared  
236 brightness temperatures, global rainfall rates, and analysis temperatures. Convective influence is  
237 said to occur if an air parcel is over a convective system, and its potential temperature is lower  
238 than the cloud top potential temperature. The method allows calculation both of the time to most  
239 recent convection for a given sampled air parcel, and the location of that most recent convection.

240 allowing air from African convection to be sampled, which was apparent in the CO<sub>2</sub> and methane  
241 measurements.

242 The second flight (RF02 16–17 February) occurred as the monsoon anticyclone was reforming  
243 east of Guam. There was very active convection about 7 degrees south of Guam, which undoubt-  
244 edly contributed to the substantial change in the anticyclone's position. Shortly after takeoff on

245 RF02, the primary satellite communications system for Global Hawk command and control (IN-  
246 MARSAT) was discovered to be inoperative. As a result, the aircraft was forced to stay within line  
247 of sight of the ground station on Guam. The aircraft circled in the zone next to Guam reserved for  
248 unmanned aircraft climbout and final descent for 17.5 hours providing 26 vertical profiles through  
249 the TTL. This turned out to be an interesting location to profile on this day, with a distinct double  
250 cold point temperature structure and corresponding vertical lamination in tracer concentrations  
251 that is related to the wave motions (?). TTL cirrus streaming over Guam from deep convection to  
252 the southeast was sampled much of the time on this flight. The stationary position of the aircraft  
253 over Guam allowed high time resolution sampling of an inertia-gravity wave with a peak-to-peak  
254 amplitude of about 5 K. This wave contributed to the in situ formation of observed TTL cirrus at  
255 the cold point near 17.7 km altitude. The CAST and CONTRAST aircraft (NERC BAe-146 and  
256 NSF G-5) sampled near the Global Hawk flight path on this day.

257 For the remainder of February, convection continued to strengthen just south of Guam, consistent  
258 with the onset of the active phase of the Madden Julian Oscillation (MJO). In response, the upper  
259 level anticyclone was pushed east of Guam, along with the coldest tropopause temperatures. As  
260 preparations for RF03 were underway around the beginning of March, a tropical cyclone was  
261 developing southeast of Guam. By the time of RF03 on 4–5 March, cyclone Faxai had swept  
262 northward east of Guam and briefly reached typhoon status around the time the Global Hawk  
263 sampled the TTL in the vicinity of the storm (see Figure 5). The flight path took the aircraft  
264 northwest from Guam and then along an eastbound leg just south of the cyclone. Multiple vertical  
265 profiles were executed through the outflow cirrus emanating from the cyclone. Except for a few  
266 occasions at the highest altitudes, the observed flow was from the south and southwest, so the  
267 air sampled during multiple vertical profiles was about 0.5–2 days old, having detrained from the  
268 cyclone when it was actually south of the flight track. Temperatures were sufficiently cold (the

269 coldest measured temperatures during the ATTREX Guam flights) to maintain (or reform) the  
270 outflow cirrus from the cyclone over that period of time. The TTL cirrus tops were as high as  
271 17.3 km. The flight provides an excellent case study of TTL composition perturbation by deep,  
272 organized convection.

273 The tropical cyclone sampled by RF03 marked the beginning of a shift of convection toward the  
274 southern hemisphere, a weakening of the monsoon anticyclone, and a clear eastward propagation  
275 of the MJO. In response to the shift in convection, the coldest temperatures moved into the southern  
276 hemisphere. The 6–7 March (RF04) flight took place in this environment, providing an additional  
277 survey of western Pacific TTL tracers and cirrus. The aircraft was directed south to 6°N and then  
278 flew a long, approximately constant-altitude leg at this latitude where multiple radiosonde stations  
279 are located, with the objective of characterizing wave properties with the combination of MMS  
280 and MTP measurements and the radiosondes. Because of the weakening anticyclone and shift of  
281 cold temperatures and convection to the southern hemisphere, this flight had temperatures about  
282 3 K warmer than typical of the other flights. (The minimum temperature for RF04 was about  
283 188 K.) The amount of fresh (less than 2 days) convective injection was notably less than during  
284 RF03, though there was significant convective influence about 3–5 days old from the strong MJO  
285 that had dominated the last two weeks of February. Even though temperatures were warmer in  
286 RF04 than in the other flights, some of the highest thin cirrus (up to 17.9 km) was observed on this  
287 flight.

288 The fifth local flight (RF05) on 9–10 March served as a southern survey and included consid-  
289 erable sampling in the outflow of strong convection. The goal was to reach about 20°S, but the  
290 aircraft had to turn back near 12°S due to a line of intense convection that developed at about  
291 17°S reaching the cold point tropopause at about 17 km. Tropical cyclone Lusi was developing  
292 at 15°S just east of the flight track. Cirrus with high ice water content and numerous ice crystals

293 was sampled up to the cold-point tropopause along the southernmost leg of the flight. Prevailing  
294 winds at flight level were from the east and southeast, so this air mass originated from the line of  
295 convection to the south.

296 Flight RF06 on 11–12 March served as a northern survey and was confined to latitudes north of  
297  $10^{\circ}\text{N}$ , with multiple vertical profiles on both the tropical and extra-tropical sides of the subtropical  
298 jet. Two of the profiles north of the jet extended down to 43,000 ft ( $\approx 13.1$  km) in order to sample  
299 as much of the extra-tropical lowermost stratosphere as possible. The objective of this flight was to  
300 provide tracer measurements both in the TTL and in the extratropical lower stratosphere for quan-  
301 tification of the role of in-mixing on TTL composition. As in the case for RF05, both convection  
302 and the coldest temperatures were south of the equator, so very little fresh convection was noted  
303 on this flight. A developing trough in the midlatitude western Pacific moved the boundary between  
304 midlatitude and tropical air southward, making the midlatitude air more accessible for sampling.  
305 Minimum temperatures were typically about 189 K in RF06, substantially warmer than the other  
306 flights. As had been the case since RF03, the anticyclone was east of Guam (Figure 3) resulting in  
307 northward and northwestward flow over the tropical portion of the track. Aged convective outflow  
308 from the South Pacific Convergent Zone was apparent in the tracers. Close to the end of the flight,  
309 the aircraft passed over a line of convection southeast of Guam, with cloud tops at about 15.5 km.  
310 Temperature fluctuations were observed during this passage, with the lowest temperatures of the  
311 flight observed (about 187.5 K). The aircraft was able to descend downstream of this convection  
312 and sample the outflow.

313 The transit back to AFRC provided the first opportunity to perform vertical profiling in the  
314 central Pacific (since the transit from AFRC to Guam was entirely at cruise altitude). At this time  
315 convection was reforming north of the equator, but consistent with the eastward propagation of the  
316 MJO, the convection was well east of Guam. In response to the increased northern hemisphere

317 convection, cold temperatures in the TTL moved north and occupied a large area centered on the  
318 equator and east of the convection (and east of the dateline). For the most part, the gradual climb  
319 to 17 km during the first 6 hours of the flight was in relatively warm temperatures and downstream  
320 of a large, deep convective system with cloud tops up to the cold point tropopause. During this  
321 portion of the flight, a layer of ice crystals and freshly lofted air (age about a day) was observed,  
322 with minimum temperatures of  $\simeq 192$  K. About 6 hours into the flight, as the aircraft crossed the  
323 dateline, vertical profiling in the cold pool commenced. Temperatures were 5 K colder east of the  
324 dateline, the air was considerably older (3 days to a week, depending on altitude, with the older  
325 air at higher altitudes), and substantial cirrus were observed. The transit back to AFRC provided  
326 an additional survey of TTL composition across the western and central Pacific.

#### 327 **4. Overview of ATTREX measurements**

328 It was recognized in the ATTREX planning stage that the Boreal wintertime western Pacific is  
329 a region with very high occurrence frequency of clouds in the TTL (?), and the ATTREX Guam  
330 flights provided a wealth of TTL cirrus measurements. As indicated by the Hawkeye measure-  
331 ments, the Global Hawk was inside TTL cirrus more than 34 hours during the flights from Guam.  
332 Figure 6 shows examples of ice crystal images and size distributions provided by Hawkeye. The  
333 CPI images often indicated bullet rosette habits and lack of evidence for ice crystal aggregates  
334 even on flight segments in cirrus that appeared to be associated with deep convection. The exis-  
335 tence of bullet rosettes is generally an indication of in situ nucleation and growth of ice crystals,  
336 whereas aggregates are typically observed in fresh anvil cirrus (?). The ATTREX data supports  
337 earlier results indicating that in situ nucleation and/or deposition growth of anvil ice crystals are  
338 important processes for generating and maintaining extensive cirrus shields around tropical deep  
339 convection (?).

340 As discussed above, the ATTREX DLH and NOAA-WV instruments provided accurate, precise  
341 water vapor measurements. Figure 7 shows frequency distributions of TTL relative humidity with  
342 respect to ice from the Guam flights as well as a comparison between DLH and NWV. The strong  
343 peak near  $RH_{ice}=100\%$  is expected since vapor deposition on and sublimation from cirrus ice  
344 crystals will tend to drive the water vapor concentration toward ice saturation. Consistent with ice  
345 nucleation and growth theory, substantial supersaturations with respect to ice occur frequently in  
346 the TTL (?). The observations of large ice supersaturations indicates that the dehydration of air  
347 passing through the TTL is less efficient than currently assumed in global models, and the model  
348 representations of TTL cirrus processes need to be modified to include supersaturation both in  
349 clear-sky regions and within cirrus. The agreement between relative humidities indicated by DLH  
350 and NWV is excellent, even at the very low mixing ratios encountered during the ATTREX flights.

351 One of the objectives of ATTREX was to investigate how waves affect the TTL cirrus formation  
352 and dehydration processes. RF04 flight was designed to survey horizontal wave structures and  
353 cirrus-wave relationships. An over flight at cruise altitudes of 17.5–18 km along 134–153°E at the  
354 nearly constant latitude of 6°N provided continuous vertical scans of clouds by the onboard down-  
355 looking CPL, as shown in Figure 8. Although ice particles were not detected at the flight altitudes  
356 in this segment due to warmer temperatures than other flights (or upstream regions), the CPL was  
357 able to observe a zonally varying, extensive cirrus layer below flight level. The cloud layer at  
358  $\simeq 12\text{--}16$  km appears to be associated with a 10-day Kelvin wave that was identified by spectral  
359 analysis of radiosonde data at Koror (134°E 7°N) and Chuuk (152°E 7°N). The bottom two panels  
360 of Figure 8 show 7–15 day filtered temperature anomalies at the two radiosonde sites. Koror was  
361 near the coldest phase of the Kelvin wave and Chuuk was near the beginning of the cold phase on  
362 March 6–7, suggesting that the wave had about a zonal wavenumber of 5 ( $\simeq 8,000$  km wavelength)  
363 with its peak near Koror and node near Chuuk. The change in the Kelvin wave amplitude likely

364 induced the change from a thicker persistent cloud layer in the west to a thinner broken cloud layer  
365 in the east.

366 Figure 9 shows an example of tracers measured in the vicinity of Typhoon Faxai on RF03.  
367 The CO<sub>2</sub> and CH<sub>4</sub> concentrations between 350 and 370 K potential temperatures measured on  
368 this flight (colored data points) were the highest values encountered over the tropical western  
369 Pacific. We examined surface measurements at various NOAA stations over the tropical Pacific  
370 in order to compare chemical signatures at the surface and the fresh, convectively lofted air. We  
371 find that concentrations of both CO<sub>2</sub> and CH<sub>4</sub> from Mauna Loa, HI agree well with the extreme  
372 concentrations sampled by the aircraft on this flight, suggesting rapid injection of nearby air from  
373 the tropical northern Hemisphere and little contribution from the tropical Southern Hemisphere.  
374 Also shown in Figure 9 are CO<sub>2</sub> concentrations sampled at other geographical locations and times  
375 during the ATTREX flights from Guam (gray data points). The spread in CO<sub>2</sub> concentrations  
376 below 370 K reflects inputs from both the northern and southern hemispheres. Above 370 K,  
377 we find reduced variability in CO<sub>2</sub> and a profile shape dictated by the phase of the CO<sub>2</sub> seasonal  
378 cycle, namely the gradual build up as the biosphere transitions from photosynthesis to respiration,  
379 ascending throughout the TTL over time.

380 Numerous trace gases were measured by the whole air sampler to better define the composition  
381 and variation of organic compounds in the TTL region. ATTREX measurements expanded by  
382 over an order of magnitude the available data of organic chemical composition in the TTL region.  
383 The gases that were measured included a range of C<sub>2</sub> - C<sub>4</sub> non-methane hydrocarbons, long-lived  
384 chlorofluorocarbons and hydrochlorofluorocarbons, various halogenated solvents, selected organic  
385 sulfur and nitrogen species, and a full range of halogenated methanes. Compounds of different  
386 lifetimes and source emission regions are being used to evaluate mixing, transport, and chemistry  
387 in the TTL region. A high priority for the ATTREX mission was to define the input of reactive

388 bromine to the stratosphere from both short-lived species (such as bromoform,  $\text{CHBr}_3$ ) as well as  
389 the longer lived compounds (such as halons and methyl bromide). These measurements (along  
390 with ozone) are illustrated in Figure 10. The average concentration of short-lived brominated  
391 compounds contribute approximately 18% of the total organic bromine at the tropical tropopause.  
392 The data will be used in conjunction with the BrO measurements from the DOAS instrument to  
393 examine the total bromine budget and partitioning between organic and inorganic bromine in the  
394 TTL and lower stratosphere.

## 395 **5. Summary and discussion**

396 The 2014 ATTREX deployment to Guam has provided a unique dataset of highly resolved tracer,  
397 cloud, water vapor, chemical radical, and radiation measurements in the western Pacific tropical  
398 tropopause layer. The wintertime western Pacific TTL is particularly important for controlling  
399 stratospheric composition because the coldest tropopause temperatures and strongest vertical as-  
400 cent rates occur in this region. The six Global Hawk flights from Guam provided surveys of  
401 western Pacific TTL composition, measurements in regions recently influenced by deep convec-  
402 tion, extensive sampling of TTL cirrus and relative humidity, spectrally-resolved radiative flux  
403 measurements, measurements of TTL wave characteristics, and measurements of tracer gradients  
404 between the TTL and extratropical lower stratosphere.

405 The ATTREX measurements are being used for two general types of analyses: (1) phenomeno-  
406 logical studies focused on understanding particular physical processes such as TTL transport path-  
407 ways and rates, ice cloud formation and dehydration, dynamics controlling TTL thermal structure,  
408 transport and chemical processes controlling halogen species concentrations; and (2) evaluation  
409 and improvement of global-model representations of these TTL processes. The precise, high-  
410 resolution tracer measurements in the remote western Pacific provided a wealth of information

411 about both deep convective and large-scale transport into and through the TTL. The ATTREX mea-  
412 surement suite included tracers with maritime, industrial, biomass-burning, and southern hemi-  
413 sphere sources. The unprecedented accuracy and precision of the water vapor measurements per-  
414 mits quantitative investigations of cloud processes such as ice nucleation, crystal growth, sedimen-  
415 tation, and removal of vapor in excess of saturation. The long Global Hawk flights along with the  
416 high occurrence frequency of cirrus in the western Pacific TTL resulted in accumulation of about  
417 34 hours of sampling in clouds. This extensive dataset permits statistical analyses of the cloud  
418 properties and humidity in addition to studies of particular cloud events.

419 The ATTREX data is openly available (<https://espoarchive.nasa.gov/>). However, data users are  
420 strongly encouraged to discuss the uncertainties and applicability of the measurements with the  
421 instrument leads listed in Table 1. Also, if the measurements are an important component of a  
422 scientific study, co-authorship should be offered to the instrument investigators.

423 Numerous modeling and data analysis activities based on the ATTREX data are currently under-  
424 way. The measurements are being used both for case-study process studies, such as understanding  
425 the processes leading to observed clouds and water vapor concentrations in particular regions (e.g.  
426 ??), and for statistical comparison with models. The dataset is proving beneficial for evalua-  
427 tion of global-model representations of transport, chemical processes, and cloud processes. The  
428 combined datasets from CAST (lower–middle troposphere), CONTRAST (middle–upper tropo-  
429 sphere), and ATTREX (upper troposphere–lower stratosphere) are being used to understand pro-  
430 cesses controlling short-lived organic and inorganic halogen species. The expectation is that the  
431 model improvements based on these analyses will improve the accuracy of climate predictions.

432 Although the ATTREX measurements have provided an invaluable dataset for studying TTL  
433 physical processes, a number of key measurement needs remain. Operational limits prevented  
434 the Global Hawk from sampling regions with temperatures colder than about 186 K. Trajectory

435 calculations indicate that most air parcels transiting through the TTL during Boreal wintertime  
436 experience colder temperatures. Measurements of water vapor and cloud properties at the lowest  
437 TTL temperatures would be useful for investigating dehydration processes at the point of mini-  
438 mum saturation mixing ratio. The ATTREX payload did not include aerosol measurements, and  
439 very little information about TTL aerosol composition and physical properties is available. In par-  
440 ticular, direct measurements of ice nuclei concentration and composition in the TTL are needed to  
441 definitively determine the relative importance of homogeneous and heterogeneous ice nucleation  
442 for production of TTL cirrus ice crystals.

443 The lack of suitable Global Hawk bases and cost issues prevented the originally planned AT-  
444 TREX operations in the southeast Asia region during Boreal summertime. Physical processes  
445 controlling TTL humidity, clouds, and general composition are likely very different during the  
446 summertime “warm phase” of the tropical tropopause seasonal temperature variation. In particu-  
447 lar, the summertime TTL and lower stratosphere composition appears to be dominated by convec-  
448 tion and radiative heating associated with the Asian monsoon (e.g. ???). Aircraft measurements  
449 of TTL properties and physical processes in southeast Asia during Boreal summertime would help  
450 address these issues.

451 *Acknowledgments.* We would like to thank the Global Hawk project managers, pilots, and crew.  
452 Without their hard work overcoming numerous challenges, collection of the excellent data de-  
453 scribed here would not have been possible. Additional funding from the Deutsche Forschungsge-  
454 meinschaft (DFG), grant number PF 384 12/1, in support of the DOAS measurements and data  
455 processing is acknowledged.

## 456 **References**

457 **LIST OF TABLES**

458 **Table 1.** Global Hawk Payload . . . . . 24

459 **Table 2.** ATTREX Guam Global Hawk flights . . . . . 25

TABLE 1. Global Hawk Payload

<b>Instrument</b>	<b>Investigator</b>	<b>Institution</b>	<b>Measurements</b>
<b>Remote</b>			
Cloud Physics Lidar (CPL)	M. McGill	NASA/GSFC	Aerosol/cloud backscatter
Microwave Temperature Profiler (MTP)	M. Mahoney	JPL/Caltech	Temperature profile
Differential Optical Absorption Spectrometer (DOAS)	J. Stutz, K. Pfeilsticker	UCLA/Univ. Heidelberg	O <sub>3</sub> , O <sub>4</sub> , BrO, NO <sub>2</sub> , OCIO, IO H <sub>2</sub> O, cloud properties
<b>In Situ</b>			
Diode Laser Hygrometer (DLH)	G. Diskin	NASA/LaRC	H <sub>2</sub> O vapor
NOAA Water (NW)	T. Thornberry, A. Rollins	NOAA/CIRES	H <sub>2</sub> O (vapor and total)
Hawkeye (2D-S, FCDP, CPI)	P. Lawson	Spec, Inc.	Ice crystal size distributions, habits
NOAA Ozone (NW)	R.-S. Gao	NOAA/CSD	O <sub>3</sub>
Harvard Univ. Picarro Cavity Ringdown Spectrometer (HUPCRS)	S. Wofsy	Harvard Univ.	CO <sub>2</sub> , CH <sub>4</sub> , CO
UAS Chromatograph for Tracers (UCATS)	J. Elkins	NOAA/GMD	N <sub>2</sub> O, SF <sub>6</sub> , CH <sub>4</sub> , H <sub>2</sub> , CO, O <sub>3</sub> , H <sub>2</sub> O
Solar and infrared radiometers	P. Pilewskie	Univ. of Colorado	Zenith and nadir radiative fluxes
Meteorological Measurement System (MMS)	P. Bui	NASA/ARC	Temperature, pressure, and winds
Global Hawk Whole Air Sampler (GWAS)	E. Atlas	Univ. of Miami	CFCs, halons, HCFCs, N <sub>2</sub> O, CH <sub>4</sub> , HFCs, PFCs, hydrocarbons, etc.

TABLE 2. ATTREX Guam Global Hawk flights

Flight	Date in 2014	Takeoff time, duration	Number of profiles	Science foci
Transit to Guam	16-17 January	04:16 UT, 19.9 hours	1	Transit aircraft to Guam
RF01	12-13 February	17:47 UT, 17.5 hours	30	TTL survey, cirrus sampling
RF02	16-17 February	17:18 UT, 17.7 hours	26	TTL survey, cirrus sampling
RF03	4-5 March	17:28 UT, 12.7 hours	20	Cyclone Faxai sampling, cirrus sampling
RF04	6-7 March	17:00 UT, 17 hours	24	TTL survey, wave measurements
RF05	9-10 March	15:24 UT, 19.7 hours	34	Southern survey, convective outflow
RF06	11-12 March	16:53 UT, 15.3 hours	32	Northern/midlatitude survey
Transit to AFRC	13-14 March	19:53 UT, 19.4 hours	31	Pacific tropical survey, cirrus sampling

460 **LIST OF FIGURES**

461 **Fig. 1.** Schematic depiction of TTL physical processes versus longitude and height. . . . . 28

462 **Fig. 2.** The Global Hawk unmanned aircraft system. The wing pods, one with the Hawkeye instru-  
463 ment and the other with an aerodynamic/weight dummy for balance, are visible. . . . . 29

464 **Fig. 3.** Global Hawk Guam deployment flight paths. Note that for RF02, the aircraft simply profiled  
465 over Guam. The paths of 2011 and 2013 ATTREX flights from Armstrong Flight Research  
466 Center (AFRC) in southern California are shown (white lines) for context. Average 95 hPa  
467 temperatures for the 1 February – 15 March period from ERA-Interim analyses are over-  
468 plotted, along with the incidence of infrared brightness temperatures less than 210 K (from  
469 geostationary meteorological satellites). In the tropics, 210 K is at 165 hPa, just below the  
470 mean altitude of deep convective cloud tops. The colored X’s mark the approximate position  
471 of the northern hemisphere monsoon anticyclone discussed in the text for the corresponding  
472 research flights. . . . . 30

473 **Fig. 4.** Latitude, longitude, and height coverage of ATTREX Global Hawk flights. Black curves  
474 correspond to ATTREX1 (2011) and ATTREX2 (2013); colored curves show the ATTREX3  
475 flights from Guam. The greyscale background shows the mean temperature versus latitude  
476 and height at the Guam longitude (top) and temperature versus longitude and height at the  
477 Guam latitude (bottom). Darkest shading indicates mean temperatures approaching 188 K,  
478 and lightest shading indicates mean temperatures greater than 205 K. . . . . 31

479 **Fig. 5.** RF03 flight path just south of cyclone Faxai. . . . . 32

480 **Fig. 6.** Examples of Hawkeye TTL cirrus measurements. 2D-S/FCDP size distributions in two  
481 different temperature ranges (left panel) and corresponding CPI ice crystal images (right  
482 panel) are shown. . . . . 33

483 **Fig. 7.** Top: Frequency distributions of western Pacific TTL relative humidity with respect to ice  
484 from DLH (green) and NOAA-WV (blue). Both datasets indicate a peak near 100% corre-  
485 sponding to data inside cirrus as well as common occurrence of supersaturation with respect  
486 to ice. Bottom: Ratio of DLH to NWV relative humidity with respect to ice versus the NWV  
487 relative humidity. . . . . 34

488 **Fig. 8.** Top: CPL clouds from the cruise altitude flight segment along 134–153°E at 6°N in RF04.  
489 Arrows indicate the nearby locations of radiosondes (Koror at 134°E 7°N; Chuuk at 152°E  
490 7°N). Bottom left: Radiosonde temperature anomalies filtered with 7–15 day periods for  
491 Koror. The asterisk shows the aircraft position and the thin vertical line is the view of  
492 the CPL. The dashed line indicates the top of the cirrus layer at about 16 km, which is  
493 approximately co-located with the cold-point tropopause. Bottom right: Same as bottom  
494 left, but for Chuuk. . . . . 35

495 **Fig. 9.** Vertical profiles of CO<sub>2</sub> as a function of potential temperature for the Tropical Western  
496 Pacific (15°N - 12°S) during all ATTREX flights from Guam (grey points). Highlighted in  
497 color data from the flight south of the core of Typhoon Faxai on March 4, 2014 (RF03). The  
498 color corresponds to CH<sub>4</sub> concentrations at a given CO<sub>2</sub> concentration. Also shown are 11-  
499 day averages (solid lines) and minima and maxima (dashed lines) of CO<sub>2</sub> and CH<sub>4</sub> (color)  
500 concentrations at NOAA tropical surface stations in the Northern Hemisphere (Mauna Loa,  
501 HI) and the Southern Hemisphere (American Samoa). The 11-day period extends from Feb,  
502 27 to Mar, 9 2014, which corresponds to the lifetime of the typhoon. . . . . 36

503 **Fig. 10.** Vertical profiles of selected trace gases measured in the TTL during the ATTREX Guam  
504 flights. The Whole Air Sampler data including a full suite of organic bromine compounds  
505 are shown in the left panel. The very short-lived organic bromine (VSL-Br) species include  
506  $\text{CHBr}_3$ ,  $\text{CH}_2\text{Br}_2$ ,  $\text{CH}_2\text{BrCl}$ ,  $\text{CHBr}_2\text{Cl}$ , and  $\text{CHBrCl}_2$ . Total organic bromine includes the  
507 VSL-Br species plus Halons and  $\text{CH}_3\text{Br}$ . The very short-lived organic bromine compounds  
508 contributed approximately 18% to the total organic bromine at the tropical tropopause. No  
509 systematic influence of latitude was detected in the vertical gradients. Right panel: Ozone  
510 (nmol/mol) data from the UCATS instrument. Individual points are averaged over the sam-  
511 ple integration time of the whole air samples. Ozone profiles tend to be anticorrelated with  
512 organic bromine concentrations in the TTL. . . . . 37

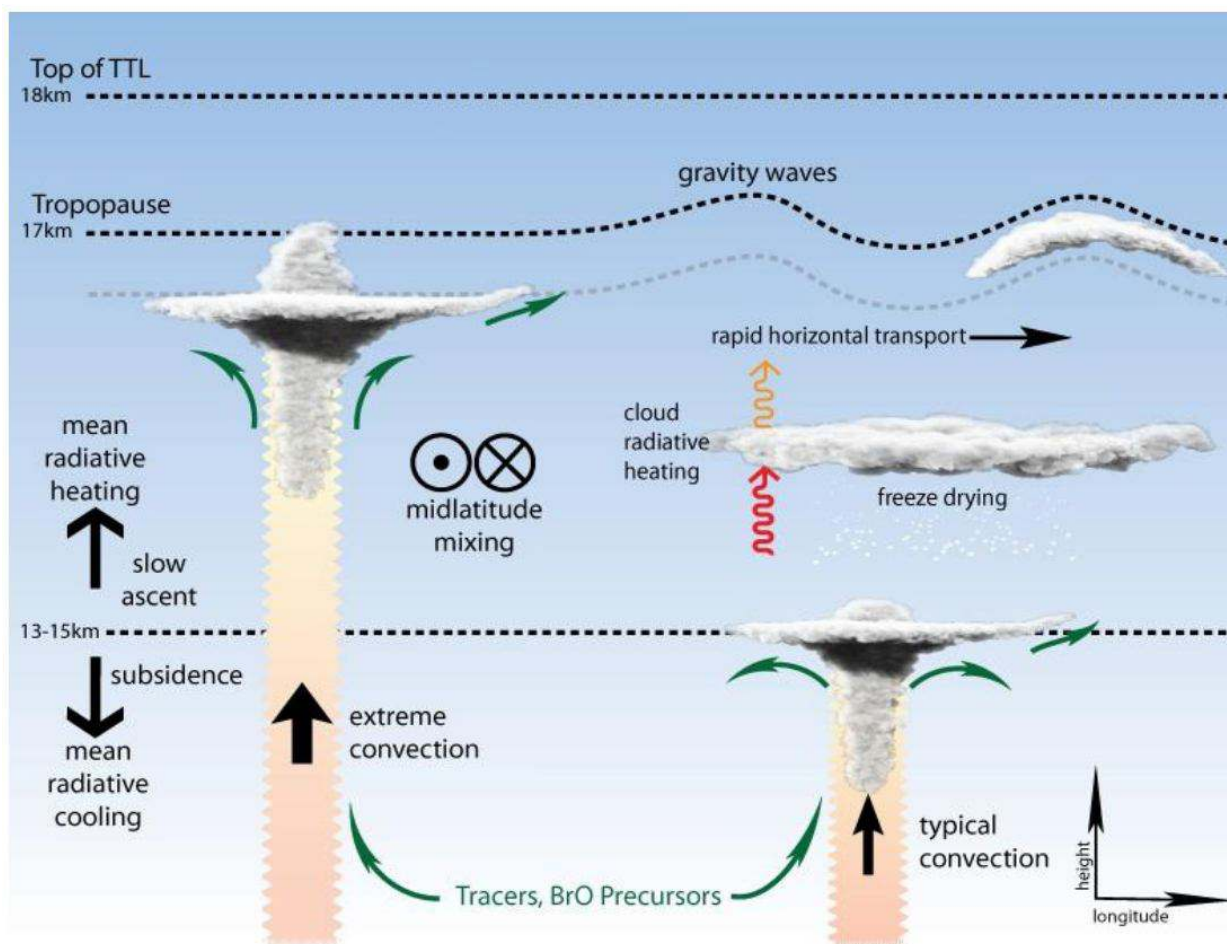
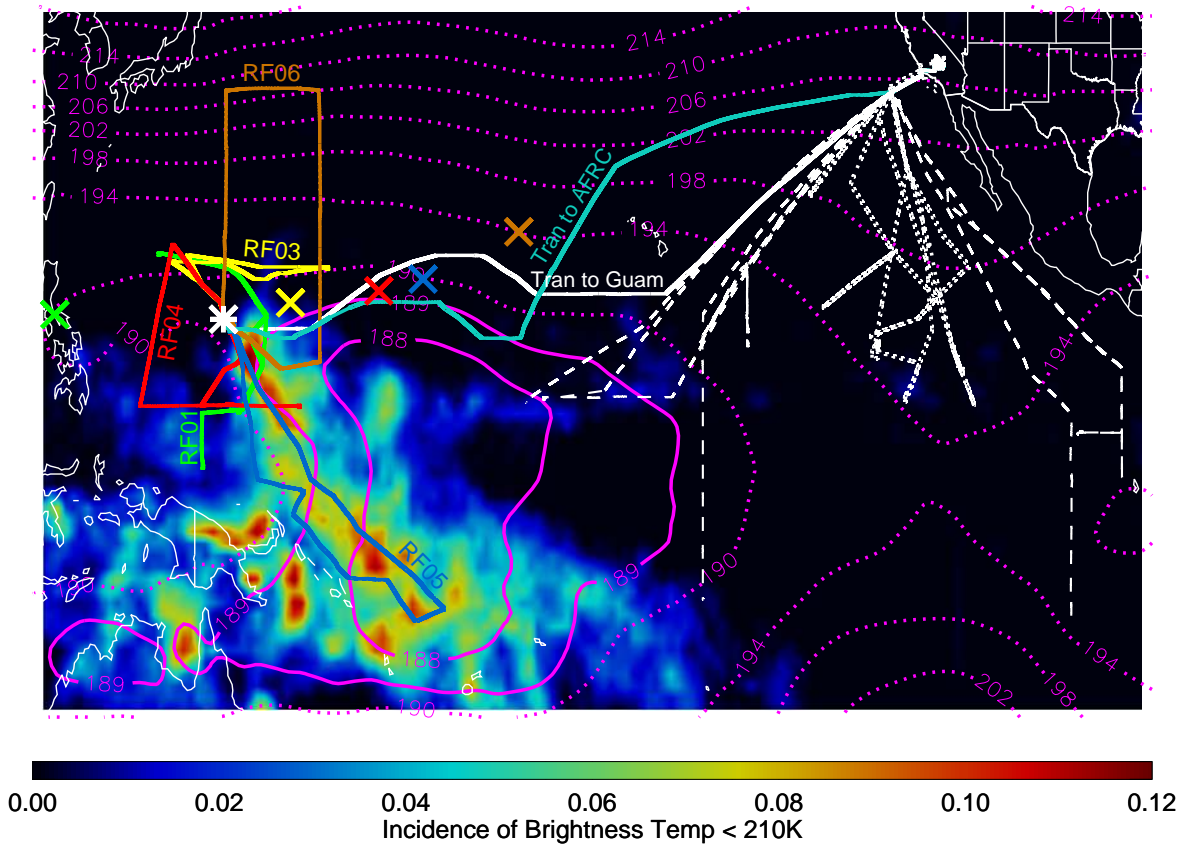


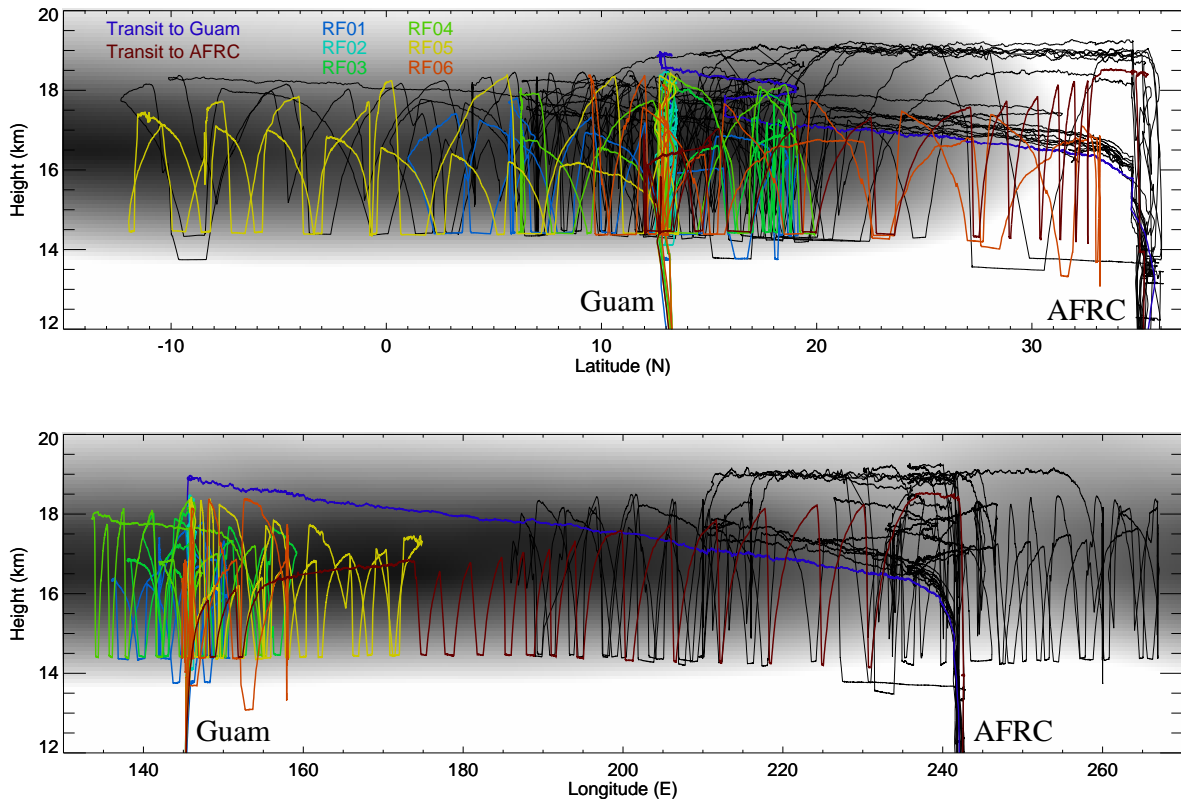
FIG. 1. Schematic depiction of TTL physical processes versus longitude and height.



513 FIG. 2. The Global Hawk unmanned aircraft system. The wing pods, one with the Hawkeye instrument and  
514 the other with an aerodynamic/weight dummy for balance, are visible.



515 FIG. 3. Global Hawk Guam deployment flight paths. Note that for RF02, the aircraft simply profiled over  
 516 Guam. The paths of 2011 and 2013 ATTREX flights from Armstrong Flight Research Center (AFRC) in south-  
 517 ern California are shown (white lines) for context. Average 95 hPa temperatures for the 1 February – 15 March  
 518 period from ERA-Interim analyses are over-plotted, along with the incidence of infrared brightness temperatures  
 519 less than 210 K (from geostationary meteorological satellites). In the tropics, 210 K is at 165 hPa, just below  
 520 the mean altitude of deep convective cloud tops. The colored X's mark the approximate position of the northern  
 521 hemisphere monsoon anticyclone discussed in the text for the corresponding research flights.



522 FIG. 4. Latitude, longitude, and height coverage of ATTREX Global Hawk flights. Black curves correspond to  
 523 ATTREX1 (2011) and ATTREX2 (2013); colored curves show the ATTREX3 flights from Guam. The greyscale  
 524 background shows the mean temperature versus latitude and height at the Guam longitude (top) and tempera-  
 525 ture versus longitude and height at the Guam latitude (bottom). Darkest shading indicates mean temperatures  
 526 approaching 188 K, and lightest shading indicates mean temperatures greater than 205 K.

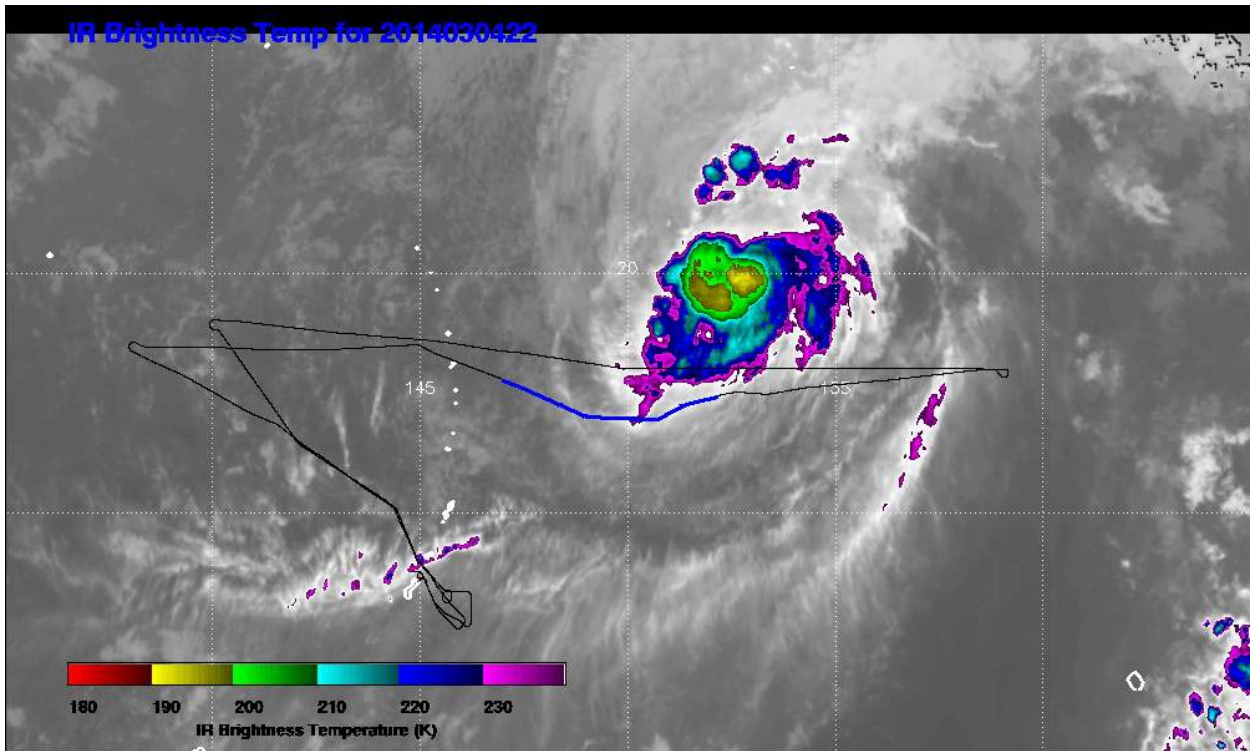
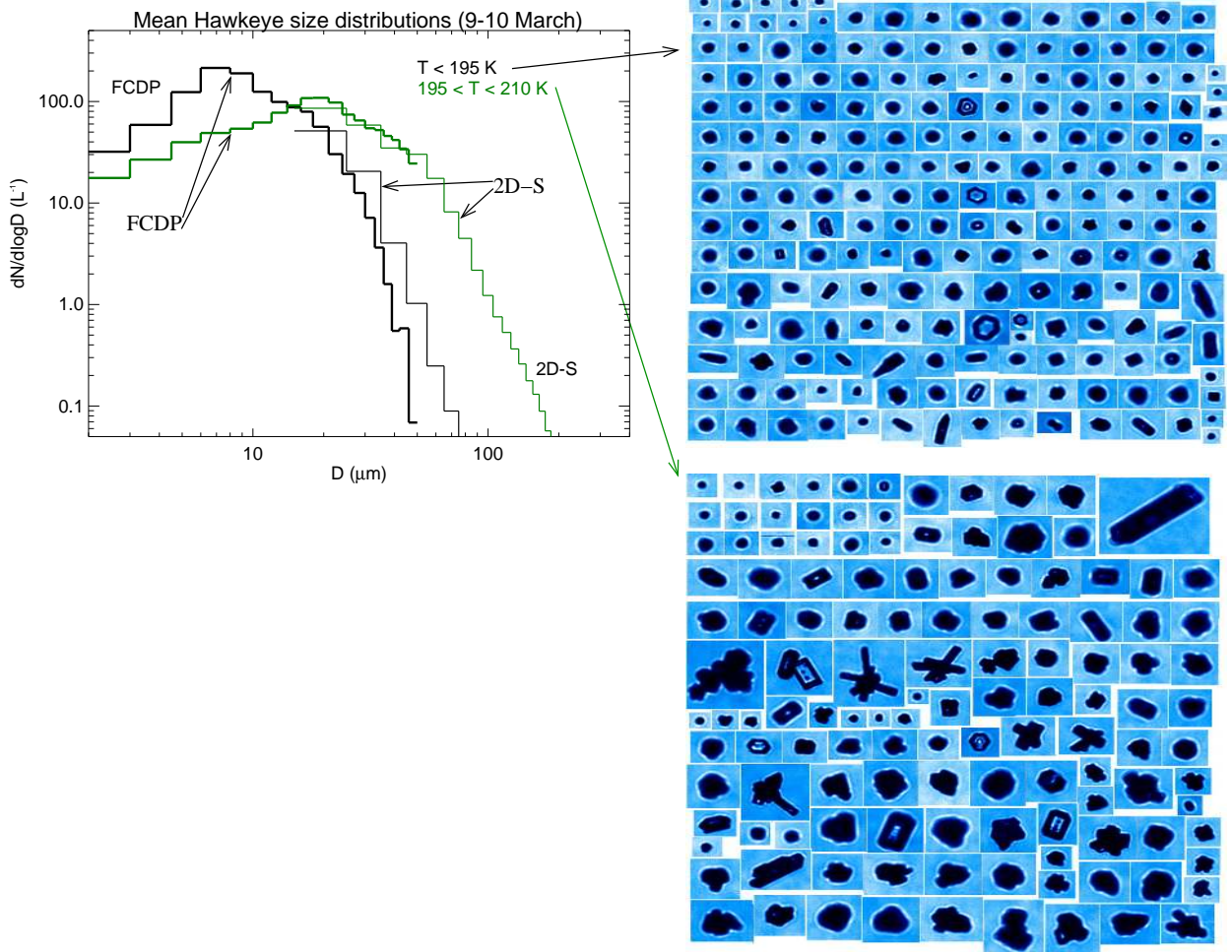
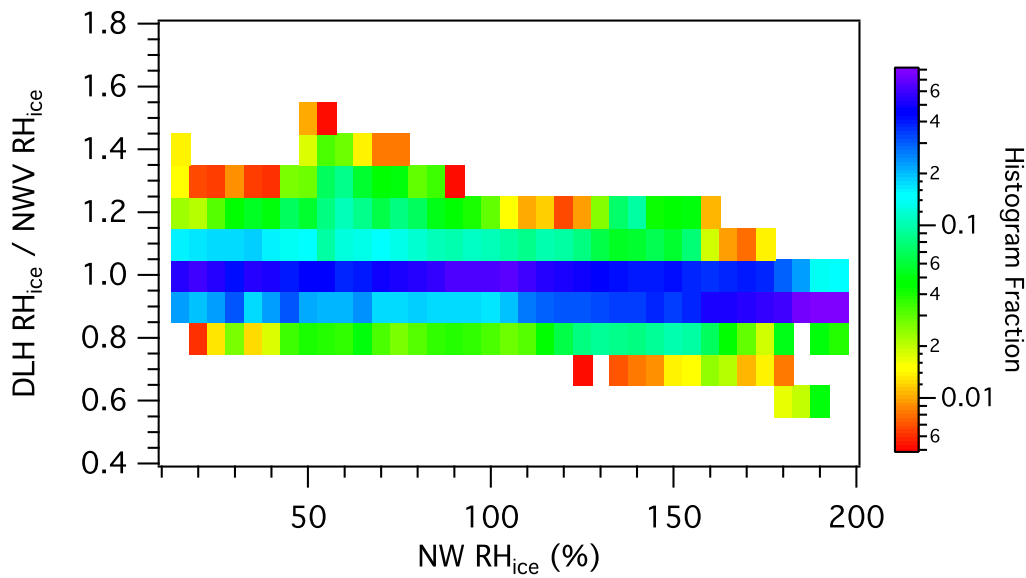
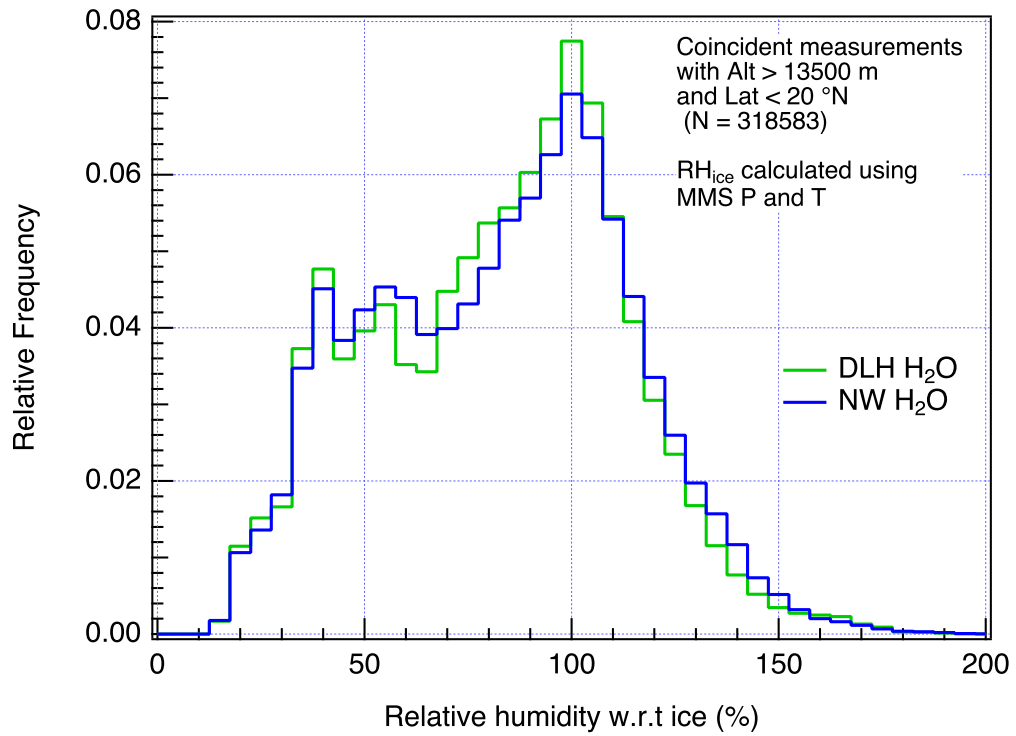


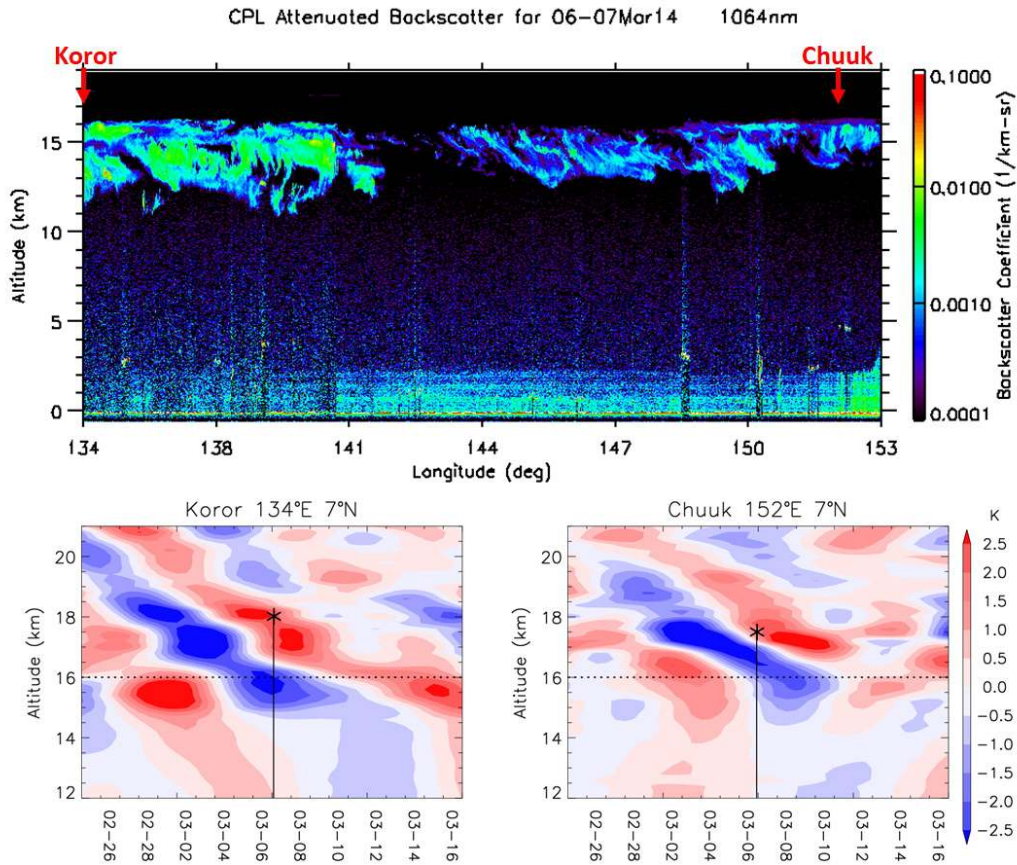
FIG. 5. RF03 flight path just south of cyclone Faxai.



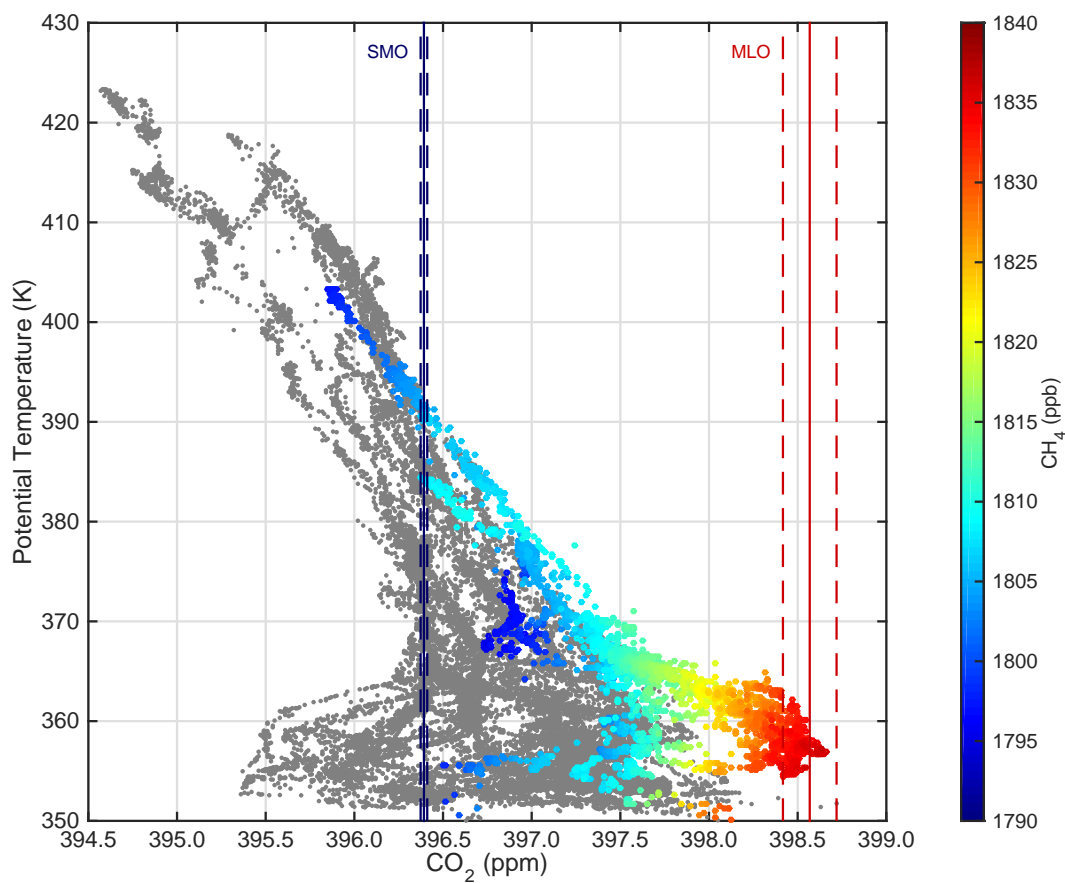
527 FIG. 6. Examples of Hawkeye TTL cirrus measurements. 2D-S/FCDP size distributions in two different  
 528 temperature ranges (left panel) and corresponding CPI ice crystal images (right panel) are shown.



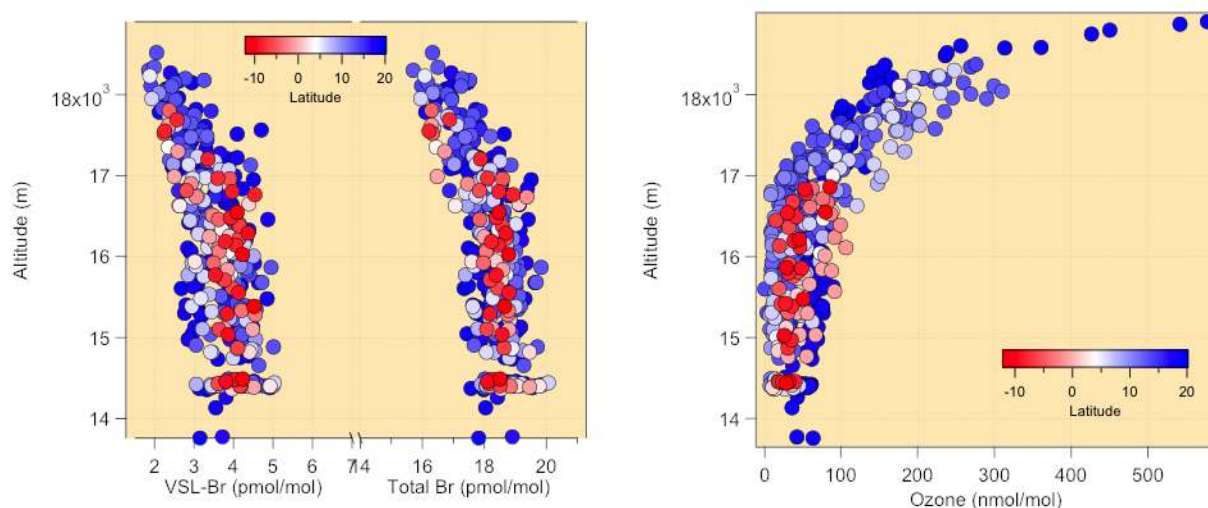
529 FIG. 7. Top: Frequency distributions of western Pacific TTL relative humidity with respect to ice from DLH  
 530 (green) and NOAA-WV (blue). Both datasets indicate a peak near 100% corresponding to data inside cirrus  
 531 as well as common occurrence of supersaturation with respect to ice. Bottom: Ratio of DLH to NWV relative  
 532 humidity with respect to ice versus the NWV relative humidity.



533 FIG. 8. Top: CPL clouds from the cruise altitude flight segment along 134–153°E at 6°N in RF04. Arrows in-  
 534 dicate the nearby locations of radiosondes (Koror at 134°E 7°N; Chuuk at 152°E 7°N). Bottom left: Radiosonde  
 535 temperature anomalies filtered with 7–15 day periods for Koror. The asterisk shows the aircraft position and the  
 536 thin vertical line is the view of the CPL. The dashed line indicates the top of the cirrus layer at about 16 km,  
 537 which is approximately co-located with the cold-point tropopause. Bottom right: Same as bottom left, but for  
 538 Chuuk.



539 FIG. 9. Vertical profiles of CO<sub>2</sub> as a function of potential temperature for the Tropical Western Pacific (15°N -  
 540 12°S) during all ATTREX flights from Guam (grey points). Highlighted in color data from the flight south of the  
 541 core of Typhoon Faxai on March 4, 2014 (RF03). The color corresponds to CH<sub>4</sub> concentrations at a given CO<sub>2</sub>  
 542 concentration. Also shown are 11-day averages (solid lines) and minima and maxima (dashed lines) of CO<sub>2</sub> and  
 543 CH<sub>4</sub> (color) concentrations at NOAA tropical surface stations in the Northern Hemisphere (Mauna Loa, HI) and  
 544 the Southern Hemisphere (American Samoa). The 11-day period extends from Feb, 27 to Mar, 9 2014, which  
 545 corresponds to the lifetime of the typhoon.



546 FIG. 10. Vertical profiles of selected trace gases measured in the TTL during the ATTREX Guam flights. The  
 547 Whole Air Sampler data including a full suite of organic bromine compounds are shown in the left panel. The  
 548 very short-lived organic bromine (VSL-Br) species include  $\text{CHBr}_3$ ,  $\text{CH}_2\text{Br}_2$ ,  $\text{CH}_2\text{BrCl}$ ,  $\text{CHBr}_2\text{Cl}$ , and  $\text{CHBrCl}_2$ .  
 549 Total organic bromine includes the VSL-Br species plus Halons and  $\text{CH}_3\text{Br}$ . The very short-lived organic  
 550 bromine compounds contributed approximately 18% to the total organic bromine at the tropical tropopause.  
 551 No systematic influence of latitude was detected in the vertical gradients. Right panel: Ozone (nmol/mol) data  
 552 from the UCATS instrument. Individual points are averaged over the sample integration time of the whole air  
 553 samples. Ozone profiles tend to be anticorrelated with organic bromine concentrations in the TTL.